

¹³C n.m.r. studies on the microstructure of piezoelectric copolymers of vinylidene cyanide

Yoshio Inoue*, Kuniaki Kawaguchi, Yoichi Maruyama, Yong Sung Jo and Riichiro Chûjô

Department of Biomolecular Engineering, Tokyo Institute of Technology, O-okayama 2-chome, Meguro-ku, Tokyo 152, Japan

and Iwao Seo and Manabu Kishimoto

Mitsubishi Petrochemical Co. Ltd, 8-3-1 Chuo, Ami-machi, Inashiki-gun, Ibaraki 300-03, Japan

(Received 19 August 1988; accepted 28 September 1988)

The microstructure of vinylidene cyanide–vinyl pivalate, vinylidene cyanide–isopropenyl acetate and vinylidene cyanide– α -methyl styrene copolymers, which were prepared by radical copolymerization, was studied by 125 MHz ¹³C nuclear magnetic resonance spectroscopy. The first copolymer shows high piezoelectricity. For the last two, piezoelectricity could not be measured because their films were too brittle. The copolymers were not found to differ greatly from each other: they were highly alternating copolymers with a non-stereoregular structure.

(Keywords: poly(vinylidene cyanide-co-vinyl pivalate); poly(vinylidene cyanide-co-isopropenyl acetate); poly(vinylidene cyanide-co- α -methyl styrene); carbon 13 n.m.r.; tacticity; microstructure; piezoelectricity)

INTRODUCTION

It is well known that crystalline polymers with large dipole moments in the side chains can exhibit high piezoelectricity if the main chain has an all-*trans* conformation (planar zigzag structure) and if the crystal displays a spontaneous polarization. A good example is poly(vinylidene fluoride) (PVDF): β -type PVDF (planar zigzag phase) has polar crystals showing large piezoelectric activity, whereas α -PVDF (3/1 helical phase) shows little piezoelectricity due to the existence of non-polar crystals^{1,2}. The crystalline copolymers of vinylidene fluoride and trifluoroethylene also have piezoelectricity as high as that of PVDF³.

In 1980, fairly high piezoelectric activity was found in a vinylidene cyanide–vinyl acetate copolymer, P(VDCN/VAc)⁴. In contrast to the fluoropolymers, this copolymer is amorphous in the piezoelectrically active state, so that X-ray analysis could give little structural information. Recently, the microstructure of P(VDCN/VAc)⁵ and vinylidene cyanide copolymers with methyl methacrylate, P(VDCN/MMA)⁶, vinyl benzoate, P(VDCN/VBz)⁷, and styrene, P(VDCN/St)⁷, were analysed successfully by nuclear magnetic resonance (n.m.r.) spectroscopy. Since the side-chain cyanide groups with large dipole moments, which would mainly contribute to the piezoelectricity, are commonly present, a similar magnitude of piezoelectric activity is expected for these four VDCN copolymers. According to this, P(VDCN/VBz) has piezoelectricity as high as that of P(VDCN/VAc)⁸, while P(VDCN/MMA)⁸ and P(VDCN/St)⁹ do not show high piezoelectricity. Molecular microstructure must be considered as one of the most important factors in determining piezoelectric activity. It was found from n.m.r. analyses^{5–7} that the

microstructures of these VDCN copolymers did not differ greatly from each other except for the chemical structure of monomeric units: they were copolymers with highly alternating and configurationally random sequences. Although the configurational randomness can explain the amorphous character of these copolymers, further investigation is required to elucidate the molecular origin of piezoelectricity of VDCN copolymers.

In this paper, the primary structure, e.g. monomer composition, monomer sequence distribution and tacticity, of another three VDCN copolymers (VDCN/vinyl pivalate, P(VDCN/PiV), VDCN/isopropenyl acetate, P(VDCN/IPA), and VDCN/ α -methyl styrene, P(VDCN/MS), are determined and compared with each other on the basis of ¹³C and ¹H n.m.r. analyses. The piezoelectric strain constant d_{31} of P(VDCN/PiV), which was poled at a temperature 10°C lower than the glass transition temperature and a field strength of 400 kV cm⁻¹ for 30 min, is 7.0 pC N⁻¹ (20°C)¹⁰. For P(VDCN/IPA) and P(VDCN/MS), we have not yet succeeded in measuring the piezoelectric property, because their films were too brittle.

EXPERIMENTAL

All VDCN copolymers used were synthesized by radical polymerization by following a similar procedure to that described elsewhere^{5,7}. The experimental details of n.m.r. measurements are essentially identical to those reported in previous papers⁷.

RESULTS AND DISCUSSION

Figures 1–3 show the 125 MHz ¹³C n.m.r. spectra of P(VDCN/PiV), P(VDCN/IPA) and P(VDCN/MS), respectively, in Me₂SO-d₆ solution. The various resonance

* To whom correspondence should be addressed

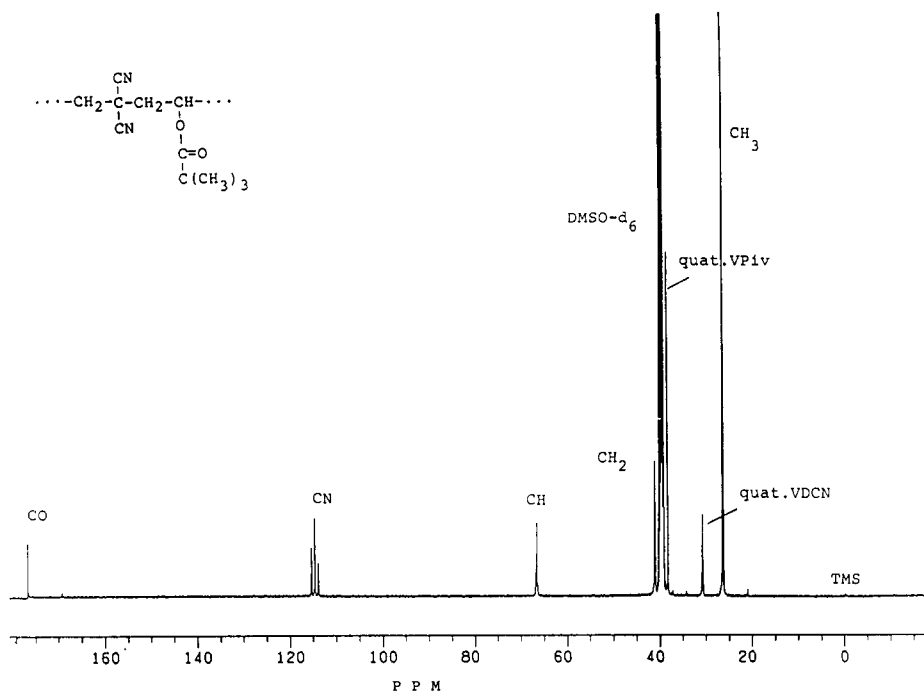


Figure 1 ¹³C n.m.r. spectrum (125 MHz) of vinylidene cyanide-vinyl pivalate copolymer in 9.5% (w/v) Me₂SO-d₆ solution at 67°C

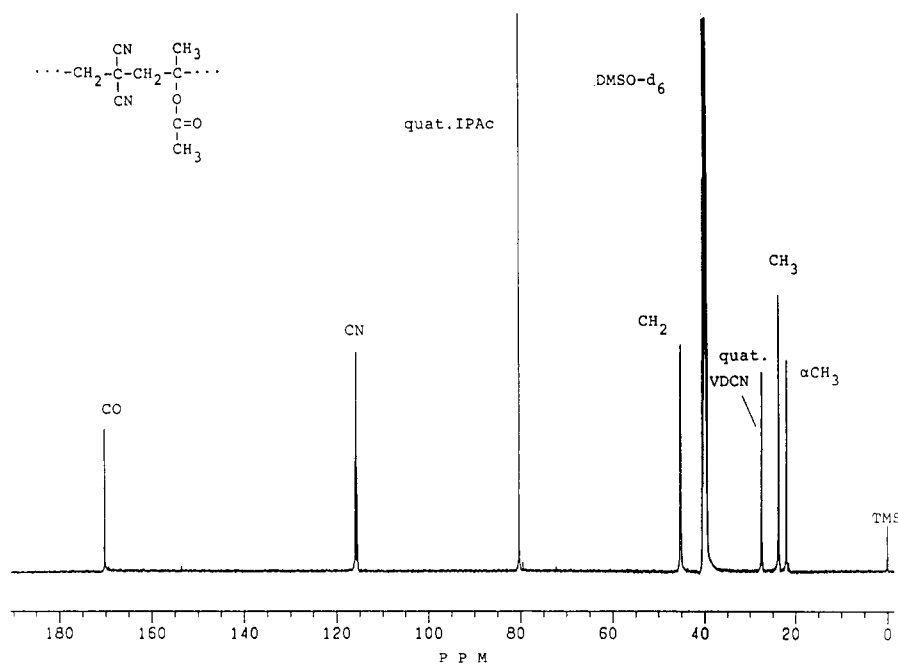


Figure 2 ¹³C n.m.r. spectrum (125 MHz) of vinylidene cyanide-isopropenyl acetate copolymer in 12.0% (w/v) Me₂SO-d₆ solution at 67°C

peaks have been assigned by comparison with those of related VDCN copolymers reported in previous papers⁵⁻⁷. All the assignments are summarized in Tables 1-3, and the details will be described later.

As each peak in the spectra of these copolymers is very sharp and simple, we may conclude that almost all monomeric units are arranged only in head-to-tail placements. As found previously for P(VDCN/VAc), P(VDCN/MMA), P(VDCN/VBz) and P(VDCN/St), the simple appearance of ¹³C spectra also indicates the strong tendency of P(VDCN/PiV), P(VDCN/IPA) and

P(VDCN/MS) to become overwhelmingly alternating copolymers.

Copolymer sequence structure

To discuss the compositional sequence distributions quantitatively, we denote the monomer sequence and the mole fractions of the monomers for P(VDCN/PiV), P(VDCN/IPA) and P(VDCN/MS) by (VDCN), (PiV), (IPA) and (MS), while those of the three dyads are given by (VDCN-VDCN), (VDCN-PiV) and (PiV-PiV) for P(VDCN/PiV), and so on. Similar notations are employed

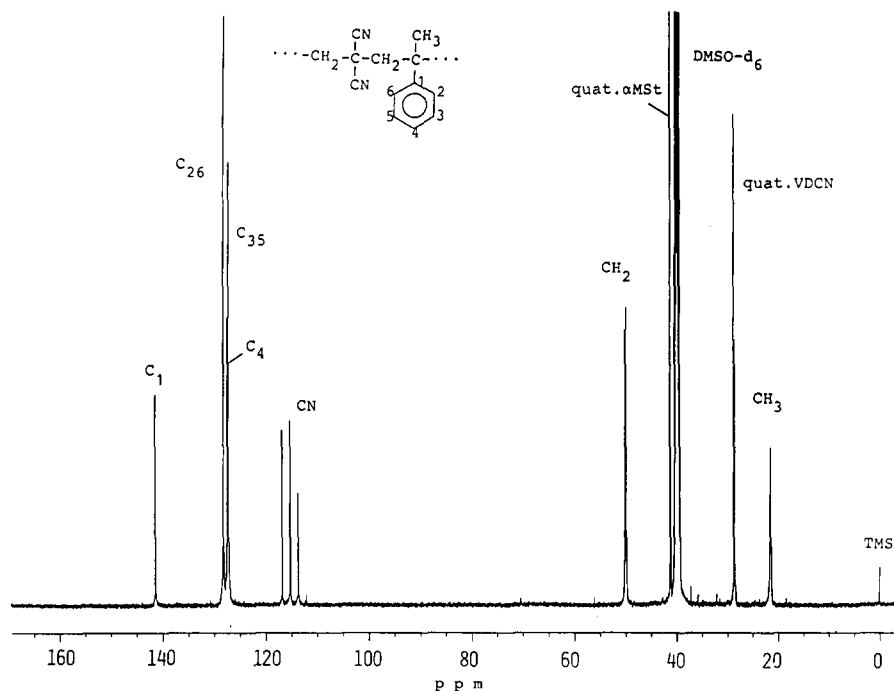


Figure 3 ^{13}C n.m.r. spectrum (125 MHz) of vinylidene cyanide- α -methylstyrene copolymer in 12.1% (w/v) $\text{Me}_2\text{SO}-d_6$ solution at 67°C

Table 1 Chemical shift assignments of P(VDCN/PiV)

Carbon	Chemical shift ^a (ppm)	Assignment
CO	176.61	(VDCN-PiV-VDCN)
CN	115.69, 114.98, 114.25 113.8-113.7	(PiV-VDCN-PiV) (VDCN-VDCN-PiV)
CH	66.64, 66.49, 66.35 66.57, 66.43	(VDCN-PiV-VDCN) (PiV-PiV-VDCN)
CH ₂	41.37, 41.33	(VDCN-PiV)
Quat. PiV	38.61 38.52, 38.47	(VDCN-PiV-VDCN) (PiV-PiV-VDCN)
Quat. VDCN	31.23-31.01	(PiV-VDCN-PiV)
CH ₃	26.21	(VDCN-PiV-VDCN)

^a Chemical shift is given with respect to internal tetramethylsilane

Table 2 Chemical shift assignments of P(VDCN/IPA)

Carbon	Chemical shift ^a (ppm)	Assignment
CO	170.31-170.22	(VDCN-IPA-VDCN)
CN	115.98, 115.70, 115.44 115.80, 115.60	(IPA-VDCN-IPA) (VDCN-VDCN-IPA)
Quat. IPA	80.26 80.37, 80.17	(VDCN-IPA-VDCN) (IPA-IPA-VDCN)
CH	45.18, 45.07	(VDCN-IPA)
Quat. VDCN	27.41-27.31	(IPA-VDCN-IPA)
CH ₃	23.68	(VDCN-IPA-VDCN)
α -CH ₃	21.92-21.91 21.37	(VDCN-IPA-VDCN) (IPA-IPA-VDCN)

^a Chemical shift is given with respect to internal tetramethylsilane

for the six triads, e.g. (VDCN-PiV-PiV), (VDCN-VDCN-PiV), (VDCN-VDCN-VDCN).

First, the monomer composition, the copolymerization parameters and the monomer sequence distribution were determined from the ^{13}C spectra. The compositional

Table 3 Chemical shift assignments of P(VDCN/MS)

Carbon	Chemical shift ^a (ppm)	Assignment
C ₆ H ₅		
C ₁	141.34, 141.29	(VDCN-MS-VDCN)
C _{2,6}	128.19	(VDCN-MS-VDCN)
C ₄	127.45	(VDCN-MS-VDCN)
C _{3,5}	127.24, 127.19, 127.16	(VDCN-MS-VDCN)
CN	116.74 115.10	(MS-VDCN-MS)
	113.62 113.44, 112.02	(VDCN-VDCN-MS)
CH ₂	50.02, 49.84	(MS-VDCN)
Quat. MS	41.23-41.20 41.33-41.30	(VDCN-MS-VDCN) (MS-MS-VDCN)
Quat. VDCN	28.65-28.42	(MS-VDCN-MS)
CH ₃	21.60, 21.47, 21.35	(VDCN-MS-VDCN)

^a Chemical shift is given with respect to internal tetramethylsilane

information concerning the dyad and triad sequences could be obtained from several resonances, the assignments of which are shown in *Tables 1-3*. For example, the composition of VDCN-centred triad sequences was estimated from the cyanide carbon resonances. The magnified cyanide resonance of P(VDCN/PiV) is shown in *Figure 4*, the features of which are very similar to those of previously reported VDCN copolymers⁵⁻⁷. Similar spectra were also observed for P(VDCN/IPA) (not shown) and P(VDCN/MS) (shown in *Figure 5*). By taking into consideration that previously reported VDCN copolymers have highly alternating sequences, the three main split peaks appearing in *Figure 4* correspond to the (PiV-VDCN-PiV) triad structure and the weak resonance appearing at 113-114 ppm from internal reference tetramethylsilane to the (VDCN-VDCN-PiV) triad. The three splits in the main VDCN-centred cyanide resonance originate from the effect of tactic structure that will be discussed later. The fraction of the VDCN homosequence

must be insignificant for the three copolymers investigated here, as any resonance corresponding to the (VDCN-VDCN-VDCN) triad sequence⁵ could not be detected. This result is in accord with the report that the VDCN homosequence is subject to chain scission by atmospheric moisture at ambient temperature¹¹.

The fractions of VDCN-centred triads were estimated from the relative peak intensities. Similarly, the fraction of X-centred triad sequence, i.e. (VDCN-X-VDCN), (VDCN-X-X) and (X-X-X), could be estimated from the corresponding resonances of X-monomeric unit,

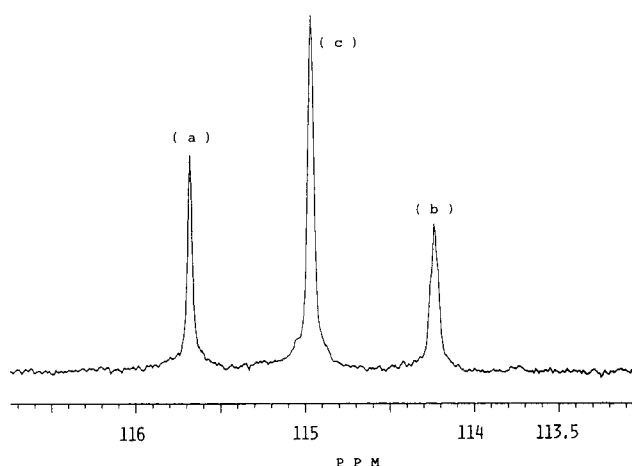


Figure 4 Expanded spectrum of the cyanide carbon resonance region of Figure 1

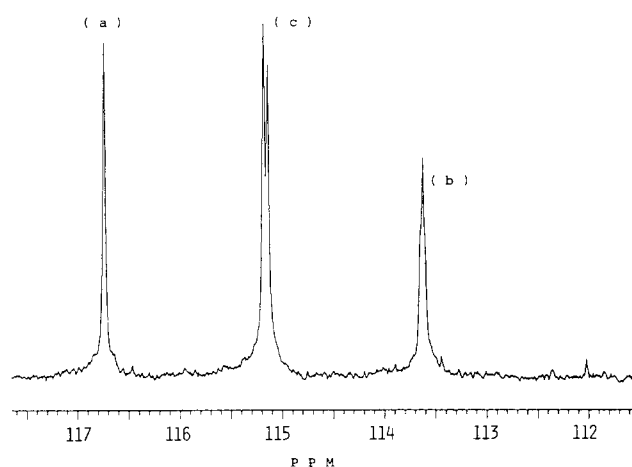


Figure 5 Expanded spectrum of the cyanide carbon resonance region of Figure 3

where X indicates PiV, IPA and MS. The resonances of X-X-X homosequences were not detected either. The observed mole fractions for the six compositional triads of three copolymers are shown in Table 4.

From the results of composition with respect to the VDCN-centred and X-centred triads, we can calculate copolymerization parameters, i.e. conditional probabilities P_{12} and P_{21} , monomer reactivity ratios r_1 and r_2 , and number average sequence lengths \bar{N}_1 and \bar{N}_2 ^{5,6}. Here subscripts 1 and 2 indicate monomeric units VDCN and X respectively. Further, the compositions of three possible dyad sequences and the monomer compositions can be also estimated by using the above triad compositional distributions. The monomer compositions can be obtained independently from ¹H n.m.r. spectra (not shown) and the results are in good agreement with those from ¹³C n.m.r. The values of copolymerization parameters as well as those of monomer compositions are given in Table 5 for the three copolymers. From the facts that the values of the two conditional probabilities P_{12} and P_{21} as well as those of the two number average sequence lengths are close to unity, that the monomer reactivity ratios are almost zero, and that the monomer composition ratio is actually 1:1 for respective copolymers, we know that the three copolymers investigated here have a highly alternating character and their sequence distributions do not differ greatly.

Using the monomer compositions as well as the conditional probabilities, the mole fractions for all six triads can be calculated⁵⁻⁷. The calculated results are also summarized in Table 4. It can be seen in this table that the fractions of alternating triads, i.e. (X-VDCN-X) and (VDCN-X-VDCN), exceed more than 0.95 for respective copolymers, indicating again the alternating character.

Configurational structure

To analyse the tactic structure, the concept of

Table 5 Copolymerization parameters and monomer compositions in P(VDCN/PiV), P(VDCN/IPA) and P(VDCN/MS)

Parameter	P(VDCN/PiV)	P(VDCN/IPA)	P(VDCN/MS)
P_{12}	0.988	0.993	0.992
P_{21}	0.975	0.991	0.980
r_1	0.012	0.007	0.009
r_2	0.026	0.009	0.021
\bar{N}_1	1.012	1.007	1.009
\bar{N}_2	1.026	1.009	1.021
[VDCN]	0.493	0.499	0.494
[X] ^a	0.507	0.501	0.506

^a X represents PiV, IPA or MS

Table 4 Calculated and observed fractions of VDCN, PiV, IPA and MS-centred triads in P(VDCN/PiV), P(VDCN/IPA) and P(VDCN/MS)

Triad	P(VDCN/PiV)		P(VDCN/IPA)		P(VDCN/MS)	
	Calc.	Obs.	Calc.	Obs.	Calc.	Obs.
(VDCN-VDCN-VDCN)	0.0001	N.d. ^b	0.0000	N.d.	0.0004	N.d.
(VDCN-VDCN-X) ^a	0.0231	0.024	0.0137	0.014	0.0168	0.017
(X-VDCN-X)	0.9768	0.976	0.9862	0.986	0.9830	0.983
(X-X-X)	0.0005	N.d.	0.0003	N.d.	0.0004	N.d.
(X-X-VDCN)	0.0449	0.046	0.0365	0.037	0.0402	0.041
(VDCN-X-VDCN)	0.9546	0.954	0.9632	0.963	0.9592	0.959

^a X represents PiV, IPA or MS

^b N.d., not detected

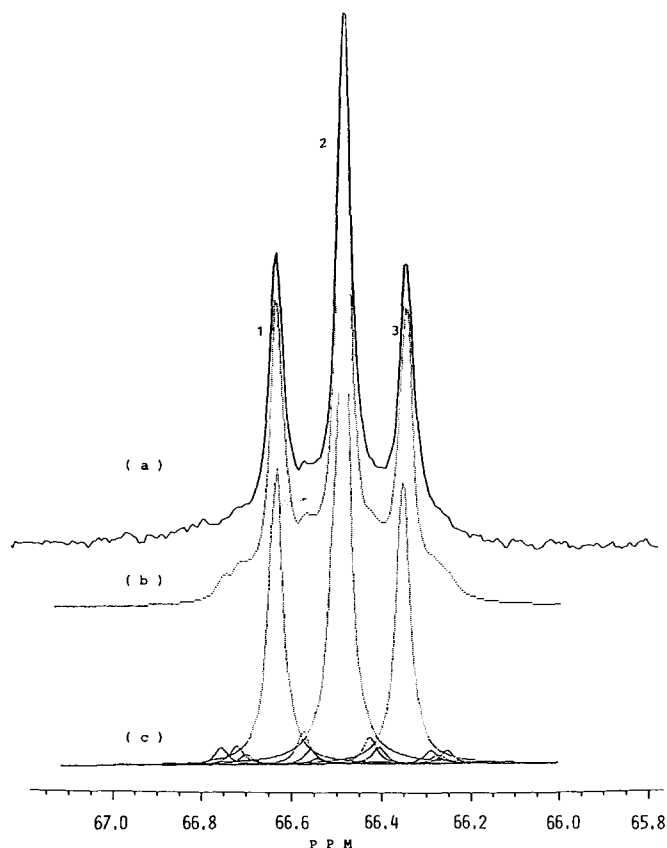
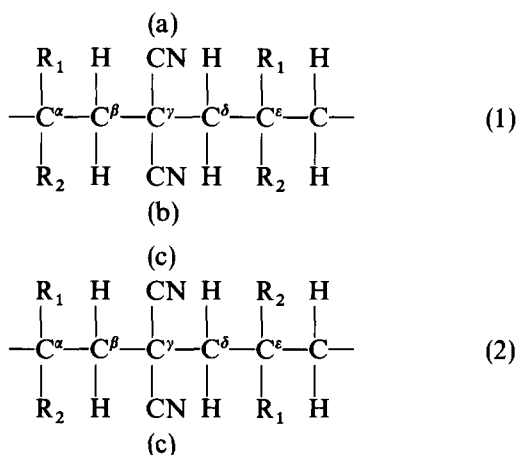


Figure 6 Expanded spectrum of the methine carbon resonance region of Figure 1. (a) Observed spectrum; (b) spectrum reproduced from resolved components; (c) results of curve resolution. 1, $m_e m_e$; 2, $m_e r_e + r_e m_e$; 3, $r_e r_e$

ϵ -tacticity defined in previous papers⁵⁻⁷ is useful. If we consider VDCN-X as a repeating monomeric unit in the alternating sequence of P(VDCN/X), two different segment structures in a dyad sense are possible:



where R_1 and R_2 are H and $-\text{OCOC}(\text{CH}_3)_3$ for P(VDCN/PiV), $-\text{CH}_3$ and $-\text{OCOCH}_3$ for P(VDCN/IPA) and $-\text{CH}_3$ and $-\text{C}_6\text{H}_5$ groups for P(VDCN/MS), respectively. Here, the tacticities in formulae (1) and (2) are defined as ϵ -isotactic and ϵ -syndiotactic, respectively. The relative tactic enchainment in formula (1) is defined as m_e (ϵ -meso), and that in formula (2) as r_e (ϵ -racemo).

Figures 4 and 5 show the expanded resonances for the cyanide carbon region of P(VDCN/PiV) and P(VDCN/MS), respectively. The splitting of respective cyanide carbon resonances of the (X-VDCN-X) triad into

three peaks, (a), (b) and (c), is caused by the ϵ -tactic enchainment. In formulae (1) and (2), considering that the cyanide carbons (a) and (b) are magnetically non-equivalent while cyanide carbons (c) are magnetically equivalent, the appearance of three peaks in the cyanide carbon resonance is reasonable. Three peaks, (a), (b) and (c), are assigned to the carbons denoted by (a), (b) and (c) in formulae (1) and (2), respectively. Although the assignments of (a) and (b) carbons are not yet clearly verified, it is considered that the resonance of carbon (b) appears at a higher field region than that of (a), which may be similar to the case of other VDCN copolymers and styrene-methyl methacrylate copolymer, where the cosyndiotactic peak has been assigned at a higher field than the cosyndiotactic peak^{5-7,12,13}. Apparently, the peak at intermediate field is assigned as the resonance of carbons (c). It is interesting to note that the centre peak of the cyanide carbon resonance of P(VDCN/MS) shows more fine splitting, reflecting pentad configuration.

The ϵ -isotacticity σ_ϵ is calculated from the following equation:

$$\sigma_\epsilon = \frac{(a) + (b)}{(a) + (b) + (c)}$$

where (a), (b) and (c) are the relative intensities of the corresponding cyanide carbon resonances. The calculated values of σ_ϵ for P(VDCN/PiV), P(VDCN/IPA) and P(VDCN/MS) are 0.519, 0.516 and 0.536, respectively. These values show that these copolymers are completely atactic, and are evidence that these copolymers are amorphous in the solid state.

Figure 6 shows the expanded resonance for the methine carbon region of P(VDCN/PiV), which also splits into three peaks due to the ϵ -tactic triad in the PiV-VDCN-PiV-VDCN-PiV alternating sequence. Although the assignments are also not fully clarified, the peaks are tentatively assigned to ϵ -isotactic ($m_e m_e$), ϵ -heterotactic ($m_e r_e + r_e m_e$) and ϵ -syndiotactic ($r_e r_e$) from low to high field. As this resonance includes the contribution from the methine carbons located in a VDCN-PiV-PiV sequence, the resonance was resolved into component peaks with Lorentzian line shape on a NEC PC-9801 microcomputer. The program used for this resolution includes the optimization process of the intensities, chemical shifts and line widths using a non-linear least squares method¹⁴. The results of curve resolution is also shown in Figure 6. From this analysis, the ϵ -tactic probability ratio $m_e m_e : m_e r_e + r_e m_e : r_e r_e$ is estimated to be 0.262:0.488:0.260. If one assumes a terminal Bernoullian control model with a single parameter σ_ϵ as a stereospecific polymerization mechanism, the ϵ -tactic probability ratio is expected to be $(1 - \sigma_\epsilon)^2 : 2\sigma_\epsilon(1 - \sigma_\epsilon) : \sigma_\epsilon^2$. Using the σ_ϵ value of 0.519 determined from the cyanide carbon resonance of P(VDCN/PiV), this ratio is calculated to be 0.269:0.499:0.231, which is in good agreement with the observed ratio. Figure 7 shows the expanded resonance for the backbone quaternary carbon region of P(VDCN/PiV), indicating clearly six peaks due to the six possible ϵ -tactic tetrads. This resonance was also resolved on the computer and six peaks are tentatively assigned on the basis of relative intensities predicted from the Bernoullian statistics, as shown in Figure 7. The split of the peak due to the difference of tactic structure can be also seen in the resonance of methylene carbons for P(VDCN/PiV), and in those of several carbons for

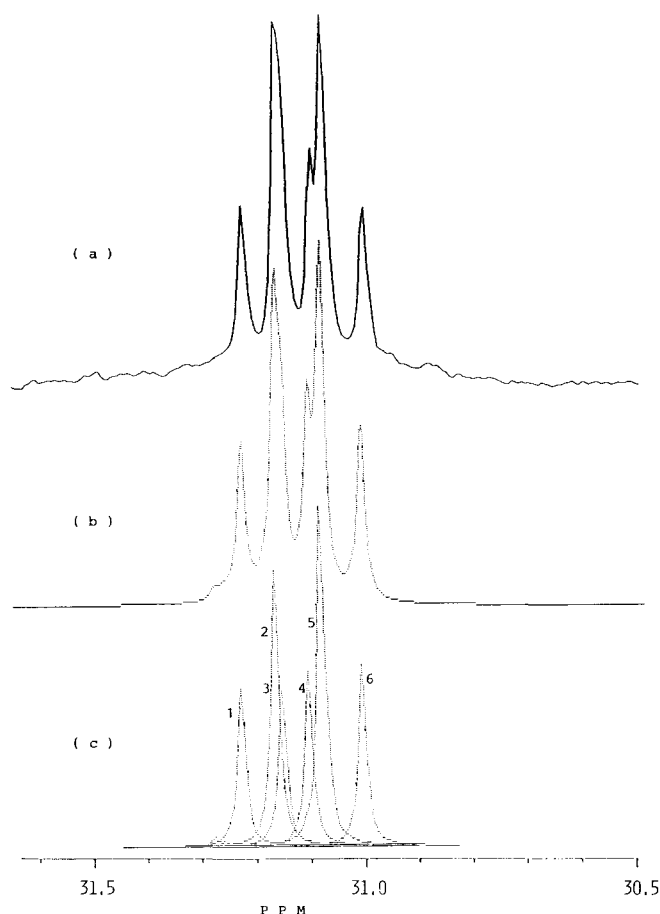


Figure 7 Expanded spectrum of the backbone quaternary carbon resonance region of Figure 1. (a) Observed spectrum; (b) spectrum reproduced from resolved components; (c) results of curve resolution. 1, $r_e r_e r_e$; 2, $m_e r_e r_e + r_e r_e m_e$; 3, $r_e m_e r_e$; 4, $m_e r_e m_e$; 5, $m_e m_e r_e + r_e m_e m_e$; 6, $m_e m_e m_e$

Table 6 Signal assignments and relative intensities in alternating fractions of P(VDCN/PiV)

Carbon	Chemical shift ^a (ppm)	Assignment	Relative intensity	
			Obs.	Calc. ^b
CN	115.67	ϵ -isotactic	0.279	—
	114.98	ϵ -syndiotactic	0.481	—
	114.25	ϵ -isotactic	0.240	—
CH	66.64	$m_e m_e$	0.262	0.269
	66.49	$m_e r_e + r_e m_e$	0.488	0.499
	66.35	$r_e r_e$	0.260	0.231
CH ₂	41.37	m_e	0.546	0.519
	40.33	r_e	0.454	0.481
Quat. VDCN	31.01	$m_e m_e m_e$	0.140	0.1398
	31.08	$m_e m_e r_e + r_e m_e m_e$	0.264	0.2591
	31.11	$m_e r_e m_e$	0.136	0.1296
	31.15	$r_e m_e r_e$	0.123	0.1201
	31.17	$m_e r_e r_e + r_e r_e m_e$	0.214	0.2402
	31.23	$r_e r_e r_e$	0.123	0.1113

^a Chemical shift is given with respect to internal tetramethylsilane

^b Values calculated on the assumption of Bernoullian statistics probability $\sigma_e = 0.519$, which is estimated from the cyanide carbon resonance

P(VDCN/IPA) and P(VDCN/MS). The observed values of tacticity in alternating sequence of P(VDCN/PiV), P(VDCN/IPA) and P(VDCN/MS) are listed in Tables 6, 7 and 8, respectively. These tables also show the values calculated on the basis of the Bernoullian model,

which describes well, on the whole, the tactic structure of the three VDCN copolymers.

CONCLUSION

Monomer composition, comonomer sequence distribution and tacticity can be determined by ¹³C n.m.r. spectroscopy for P(VDCN/PiV), P(VDCN/IPA) and P(VDCN/MS). The conclusion derived for other VDCN copolymers in previous papers, that the characteristics of the microstructures of radically polymerized VDCN copolymers do not differ greatly from each other, is confirmed: the three VDCN copolymers investigated in this paper have highly alternating and configurationally random sequences. Thus the piezoelectricity of VDCN copolymers could not be explained by a direct connection with the microstructure, and the reason why some VDCN copolymers show and others do not show high piezo-

Table 7 Signal assignments and relative intensities in alternating fractions of P(VDCN/IPA)

Carbon	Chemical shift ^a (ppm)	Assignment	Relative intensity	
			Obs.	Calc. ^b
CN	115.98	ϵ -isotactic	0.274	—
	115.70	ϵ -syndiotactic	0.484	—
	115.44	ϵ -isotactic	0.243	—
CH ₂	45.18	m_e	0.516	0.516
	45.07	r_e	0.484	0.484
Quat. VDCN	27.41	$r_e m_e r_e$	0.145	0.121
	27.38	$m_e m_e r_e + r_e m_e m_e$	0.221	0.258
	27.36	$r_e r_e r_e$	0.122	0.113
	27.35	$m_e m_e m_e$	0.152	0.138
	27.33	$m_e r_e r_e + r_e r_e m_e$	0.204	0.242
	27.31	$m_e r_e m_e$	0.158	0.129

^a Chemical shift is given with respect to internal tetramethylsilane

^b Values calculated on the assumption of Bernoullian statistics probability $\sigma_e = 0.516$, which is estimated from the cyanide carbon resonance

Table 8 Signal assignments and relative intensities in alternating fractions of P(VDCN/MS)

Carbon	Chemical shift ^a (ppm)	Assignment	Relative intensity	
			Obs.	Calc. ^b
C _{3.5} (phenyl)	127.24	$r_e r_e$	0.224	0.215
	127.19	$m_e r_e + r_e m_e$	0.470	0.497
	127.16	$m_e m_e$	0.210	0.287
CN	116.74	ϵ -isotactic	0.255	—
	115.18–			
	115.14	ϵ -syndiotactic	0.464	—
CH ₂	113.62	ϵ -isotactic	0.280	—
	50.02	r_e	0.479	0.464
	49.84	m_e	0.521	0.536
Quat. VDCN	28.65	m_e	0.545	0.536
	28.46	$m_e r_e m_e$	0.136	0.134
	28.44	$m_e r_e r_e + r_e r_e m_e$	0.222	0.230
	28.42	$r_e r_e r_e$	0.097	0.100
	21.60	$m_e m_e$	0.309	0.287
CH ₃	21.47	$m_e r_e + r_e m_e$	0.489	0.497
	21.35	$r_e r_e$	0.202	0.215

^a Chemical shift is given with respect to internal tetramethylsilane

^b Values calculated on the assumption of Bernoullian statistics probability $\sigma_e = 0.536$, which is estimated from the cyanide carbon resonance

electricity should be found in factors other than the microstructure. To attain high piezoelectric activity, VDCN copolymers must be subjected to poling treatments under high d.c. electric field. Under this treatment, the C–CN dipoles of VDCN units can rotate to align themselves in one direction, producing a large resultant dipole moment and so high piezoelectric activity. This suggests that the important factors determining degree of piezoelectric activity are chain conformation^{15,16} and chain flexibility^{17–19}. Both factors depend not only on the chemical structure but also on the microstructure. The X monomeric unit inserted alternately between VDCN units is thought to facilitate the rotation of the main chain by reducing a strong dipolar interaction between the cyanide groups. The bulkiness of the side chain of the X unit also influences the main-chain flexibility. Further work on the molecular origin of high piezoelectric activity of P(VDCN/PiV) is in progress.

REFERENCES

- 1 Lovinger, A. J., Davis, G. T., Furukawa T. and Broadhurst, M. G. *Macromolecules* 1982, **15**, 323
- 2 Davis, G. T., Furukawa, T. and Broadhurst, M. G. *Macromolecules* 1983, **16**, 1855
- 3 Uchidoi, M., Iwamoto, T., Iwata, K. and Tamura, M. *Rep. Prog. Polym. Phys. Jpn.* 1979, **22**, 345
- 4 Miyata, S., Yoshikawa, M., Tasaka, S. and Ko, M. *Polym. J.* 1980, **12**, 857
- 5 Jo, Y. S., Inoue, Y., Chûjô, R., Saito, K. and Miyata, S. *Macromolecules* 1985, **18**, 1850
- 6 Maruyama, Y., Jo, Y. S., Inoue, Y., Chûjô, R., Tasaka, S. and Miyata, S. *Polymer* 1987, **28**, 1087
- 7 Inoue, Y., Kashiwazaki, A., Maruyama, Y., Jo, Y. S., Chûjô, R., Seo, I. and Kishimoto, M. *Polymer* 1988, **29**, 144
- 8 Tasaka, S., Miyasato, K., Yoshikawa, M., Miyata, S. and Ko, M. *Ferroelectrics* 1984, **57**, 267
- 9 Kishimoto, M., Nakajima, K. and Seo, I. unpublished data
- 10 Okutani, T., Tasaka, T., Miyata, S. and Seo, I. *Polymer Prepr. Jpn.* 1987, **36**, 1064
- 11 Gilbert, H., Miller, F. F., Averill, S. J., Schmidt, R. F., Stewart, F. D. and Trumbull, H. L. *J. Am. Chem. Soc.* 1954, **76**, 1074
- 12 Hirai, H., Koinuma, H., Tanabe, T. and Takeuchi, K. *J. Polym. Sci., Polym. Chem. Edn.* 1979, **17**, 1339
- 13 Ebdon, J. R., Huckerby, T. N. and Khan, I. *Polym. Commun.* 1983, **24**, 162
- 14 Hayashi, T., Inoue, Y., Chûjô, R. and Asakura, T. *Polymer* 1988, **29**, 138
- 15 Jo, Y. S., Inoue, Y. and Chûjô, R. *Makromol. Chem. Makromol. Symp.* 1986, **5**, 167
- 16 Jo, Y. S., Sakurai, M., Inoue, Y., Chûjô, R., Tasaka, S. and Miyata, S. *Polymer* 1987, **28**, 1583
- 17 Jo, Y. S., Maruyama, Y., Inoue, Y., Chûjô, R., Tasaka, S. and Miyata, S. *Polym. J.* 1987, **19**, 769
- 18 Jo, Y. S., Maruyama, Y., Inoue, Y., Chûjô, R., Tasaka, S. and Miyata, S. *J. Polym. Sci., Polym. Phys. Edn.* 1988, **26**, 463
- 19 Inoue, Y., Jo, Y. S., Kashiwazaki, A., Maruyama, Y., Chûjô, R., Seo, I. and Kishimoto, M. *Polym. Commun.* 1988, **29**, 105